Flux-flow-induced giant magnetoresistance in all-amorphous superconductor-ferromagnet hybrids

C. Bell, S. Turşucu, and J. Aarts

Magnetic and Superconducting Materials Group, Kamerlingh Onnes Laboratorium, Universiteit Leiden, Leiden, The Netherlands

We present magnetoresistance measurements on all-amorphous ferromagnet (F)/superconductor (S) hetero-structures. The F/S/F trilayers show large magnetoresistance peaks in a small field range around the coercive field of the F layers, at temperatures within and below the superconducting transition. This is interpreted as flux flow of weakly pinned vortices induced by the stray field of Bloch magnetic domains in the F layers. Bilayers show much smaller effects, implying that the Bloch walls of the F layers in the trilayer line up and focus the stray fields. The data are used to discuss the expected minimum F-layer thickness needed to nucleate vortices.

I. INTRODUCTION

There are a number of phenomena currently under investigation which involve the combinations of superconductors (S) and ferromagnets (F). In S/F/S configurations, the superconductors can be coupled through the ferromagnetic layer, which may lead to so-called π junctions.[1] In F/S/F configurations, the superconducting transition temperature (T_c) depends on the relative orientation of the magnetization in two F layers,[2–5] which constitutes the so-called superconducting spin switch. In researching these phenomena, the question of the influence of domain structures in the F layers is often ignored. Domain walls can have various effects. For instance, superconductivity can be enhanced by domain walls, through two different mechanisms. One is that Cooper pairs sample inhomogeneous exchange interactions in the wall, or the different directions of the magnetization on the two sides of the wall, and experience less pair breaking. This was observed in bilayers of Nb and Permalloy[6] (Py) and also in Nb/Co.[7] The other mechanism comes about in ferromagnets with a preferred magnetization direction perpendicular to the plane of a superconducting film. Now, the presence of a domain wall can lead to a local reduction of the amount of flux through the superconductor, and therefore to less suppression (or relative enhancement) of superconductivity. This was demonstrated on S/F bilayers involving Nb and a ferromagnetic garnet ($BaFe_{12}O_{19}$),[8] and on S/I/F bilayers (with I an insulating barrier) and F/S/F trilayers with Pb or Nb as the S layer combined with perpendicularly magnetized Co/Pd multilayers.[9,10]

A different situation occurs when the magnetization of the ferromagnet is in plane and the magnetization in the domain wall rotates out of the plane (so-called Bloch walls). This can influence the superconductivity in the S layer if the flux from the wall creates vortices. Observations on Nb/CuNi bilayers were interpreted in this way,[11] but otherwise the problem has received little attention experimentally. Recently, the conditions for vortex formation were discussed theoretically (see Ref. 12 and references therein). In this work we present data from an experimental system well suited to observe the effects of vortices in transport measurements, consisting of a combination of an amorphous ferromagnet (a-$Gd_{19}Ni_{81}$, referred to as GdNi) and an amorphous superconductor (a-$Mo_{2.7}Ge$, called MoGe). Because of the amorphous nature

of the materials, the magnet has an extremely low switching or coercive field H_c, corresponding to an applied flux density of less than 1 mT, while the superconductor has very weak vortex pinning properties. Also, the magnetic material has a relatively high magnetization (due to the Gd atoms), which facilitates vortex formation. In F/S/F trilayers, we show the occurrence of extremely sharp resistance spikes when varying the magnetic field around H_c at temperatures near the base of the superconducting transition, which we interpret as due to flux flow. Furthermore, we find that the effect is much weaker in F/S bilayers, presumably because domain walls in both F layers tend to line up, thereby focusing the flux coming out of the walls. Such a coupling of the domain walls makes the F/S/F trilayer case different from the case of F/S bilayers. After the presentation of the data, we apply the model developed in Ref. 12 to argue that vortices can be created in the MoGe layer by the flux from the domain walls, and we discuss the requirements of vortex formation in various other S/F systems.

II. SINGLE-FILM CHARACTERISTICS

Our samples are grown on (100) oxidized Si by rf sputtering at room temperature, in a vacuum system with a base pressure below 2×10^{-6} mbar. Deposition rates were of the order of ~7.5 nm/min for the GdNi and ~8.5 nm/min for the MoGe, as calibrated from low- angle x-ray reflectivity. The compositions were found using Rutherford backscattering, and the amorphous nature of the films (i.e., the absence of crystallinity) was checked by x-ray diffraction. The bulk superconducting transition temperature T_c of our MoGe films is about 5.5 K, and such films show weak vortex pinning properties as reported on similar material grown in the same system.[13,14] Another particular property of amorphous superconductors is that the very small mean free path (also reflected in a large specific resistance of typically about 200 $\times 10^{-8}$ Ω m) leads to a large zero-temperature London (magnetic) penetration depth $\lambda_L(0)$, of order 0.7 μm. The zero-temperature coherence length $\xi(0)$ of these films is small, around 5 nm. The numbers result in a quite small value for the zero-temperature lower critical field $H_{c1}(0)$ of typically 1.3×10^3 A/m (corresponding to 1.6 mT), but in a very large value for the zero-temperature upper critical field $H_{c2}(0)$ of ~13 T.
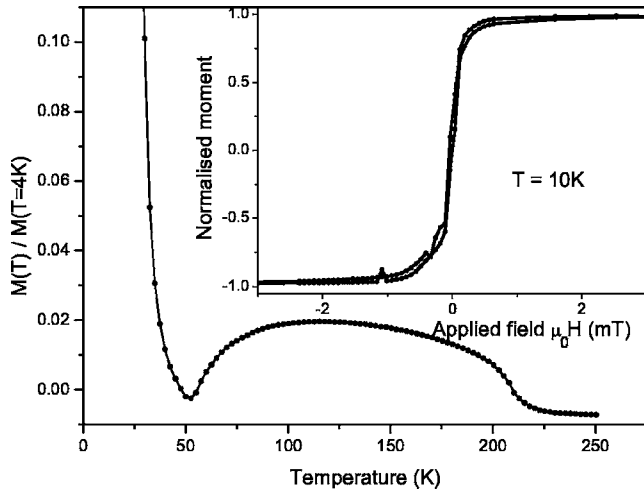
FIG. 1. Magnetic moment M, normalized to its value at 4 K, vs temperature T for a 20 nm GdNi film in an applied field of $\mu_0 H$ = 3 mT. Inset: M vs applied field $\mu_0 H$ for the same film at T = 10 K.

Amorphous GdNi belongs to a general class of ferromagnets combining a rare earth element and a transition metal element, which both carry a moment on their own subnetwork in the material. The amorphous state leads to a spatial distribution of the relative directions of the magnetic moments of both networks. If a net moment exists, the state is called sperimagnetic.[15] The moments of the two networks are coupled antiferromagnetically, and since the temperature dependence of the magnetization is different for both, there may exist a so-called compensation temperature T_{comp} where the two magnetizations cancel. The case of $Gd_{1-x}Ni_x$ is a special one. According to the literature,[15,16] the Ni atom does not possess a magnetic moment below a critical concentration $x_c \approx 0.8$ while the Gd atoms have their full S-state moment of about $7\mu_B$, and order ferromagetically. With increasing x, for $x < x_c$, the dilution effect of the nonmagnetic Ni on the Gd matrix leads to a decrease of the magnetic ordering temperature T_c down to 40 K at $x = x_c \approx 0.8$. Above x_c, a small moment appears on the Ni, antiparallel to the Gd moment, leading to a simple ferrimagnetic state. Obviously, a compensation temperature can occur only for $x > x_c$.

For our material with $x = 0.81$, we find a saturation magnetization, measured at 10 K on a film of a 75 nm, of $7.8 \pm 0.2 \times 10^5$ A/m. Assuming the full Gd moment of $7\mu_B$, this yields a small Ni moment of $-0.02\mu_B$, in good agreement with the earlier data.[17] Figure 1 shows the temperature dependence of the magnetization (normalized to the value at 4 K) of a 20 nm film, measured in an applied field of 3 mT. Clearly visible is that the magnetization already develops around 220 K, but dips again[18] to 0 at $T_{comp} = 50$ K. These values are reduced slightly for the thinner films used in the rest of this work, but the the alloy evidently orders at a much higher temperature than previously reported. It seems quite likely that T_c was mistaken for T_{comp}, possibly because of a too high applied field. The inset of Fig. 1 shows the field dependence of the magnetization, taken at 10 K. The coercive field H_c is very small in this case, less than 0.1 mT, which is a consequence of the absence of anisotropy in the
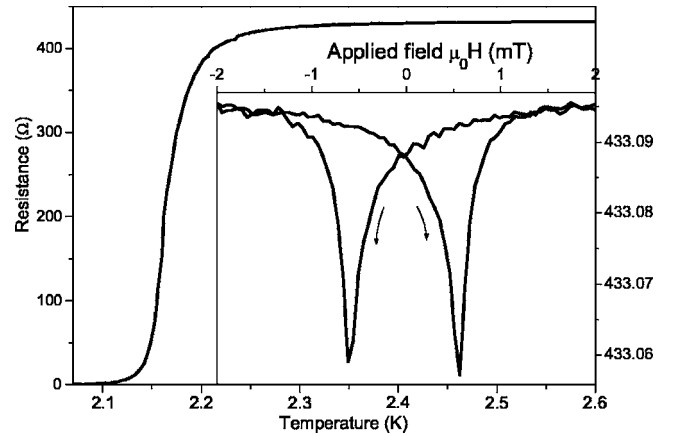

FIG. 2. Superconducting resistive transition for a patterned wire in a GdNi(11)/MoGe(21)/GdNi(11) trilayer. Inset: Magnetoresistance for $H \| I$ at 3.75 K. The arrows denote the direction of the field sweep.

Gd S state, and the lack of grain boundaries which hinder domain wall motion.

All samples were patterned with e-beam lithography and broad-beam Ar ion milling to 100-μm-wide wires for a standard four-point measurement with 1 mm between voltage contacts. The trilayer samples for which data are presented are of the form GdNi(x)/MoGe(y)/GdNi(z) with x, y, z all in nanometers, and the first of these grown on the SiO. All of the data presented are measured with the magnetic field applied in plane and (anti)parallel to the current to within a few degrees error (no precise alignment procedure was undertaken), and with a constant current of ± 100 μA unless otherwise stated.

III. RESULTS

Figure 2 shows the superconducting transition of a sample GdNi(11)/MoGe(21)/GdNi(11), with a midpoint at 2.16 K and a width (10–90 %) of 60 mK. The reduced T_c indicates a significant proximity effect from the F layers. The inset shows the behavior of the resistance R versus applied field H for $H \|$ current I at 3.75 K (above the transition). Small dips are visible around the switching field of the F layers at 0.5 mT, which is the conventional anisotropic magnetoresistance with a magnitude $\Delta R / R_{max}$ of the order of 9×10^{-5}. We observe a single peak in each quadrant, indicating that the two layers switch at the same field. Figure 3 shows $R(H)$ at 2.15 and at 2.095 K, at the base of the transition. Sweeping the field now leads to strong resistance peaks with ΔR several percent of the normal state resistance. For a related sample (with slightly lower H_c) we also plot the peak (dip) position H_{pd} of the $R(H)$ measurements through the superconducting transition (inset of Fig. 3). It is clear that H_c increases smoothly with T, and that the large magnetoresistance peaks in the transition are associated with the domain state of the F layers at H_c.

The maximum ΔR for this sample was ~ 26 Ω, representing a change of 6% of the total normal state resistance of the whole trilayer; however ΔR decreases with decreasing T and
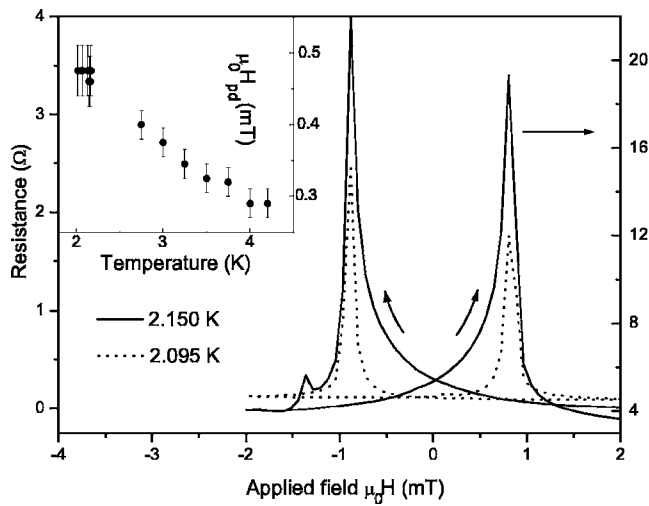
FIG. 3. Resistance vs applied field of a GdNi(11)/MoGe(21)/GdNi(11) trilayer for two temperatures within the superconducting transition as indicated. The arrows denote the direction of the field sweep. Inset: Values of the peak or dip field H_{pd} in $R(H)$ vs temperature, for a related sample with slightly lower H_c.

with this measurement current of 100 μA the voltage in the peaks passes below a 1 μV criterion at 2.03 K.

Since the resistance shows a peak in the the domain state of the F layers, we cannot interpret the data in terms of mechanisms which yield a decreased resistance (enhanced superconductivity) when the relative magnetization directions in the two F layers deviate from parallel. In principle, quasiparticle trapping could provide a mechanism for increased resistance.[6] It would then have to be argued that the domain state locally leads to antiparallel configurations between the two F layers, as was actually found in the case of F/S/F trilayers involving (La,Ca)MnO$_3$ and YBa$_2$Cu$_3$O$_7$.[19] However, in view of the weak pinning properties of the superconductor, another possibility is flux flow resistivity associated with the motion of vortices formed spontaneously above Bloch domain walls. The sample is in the force-free configuration ($H\|I$) for the applied field, but induced vortices pointing out of the plane of the sample will experience a Lorenz force due to the applied current, which can cause vortex motion across the width of the wire. To clarify this, we measured current (I)–voltage (V) characteristics on the same sample GdNi(11)/MoGe(21)/GdNi(11) at 1.8 K, well below the transition, and with the field either at $-H_c$ or slightly above $+H_c$. They are shown in Fig. 4, which also shows a sketch of the sample configuration, with the directions of applied field, current, and flux inside the F layer (including the domain wall). At this temperature we find a true supercurrent, and a gradual onset of voltage. Using a 1 μV criterion, the critical currents in the low- and high-resistive states taken from Fig. 4 are ~640 and 340 μA, respectively. Resistance peaks at this temperature therefore can still be seen, as long as the bias current is large enough to depin the vortices. This is shown in the inset of Fig. 4, where the voltage (resistance) was taken at a bias current of 1 mA.

The effect is not strongly sensitive to variation of the S- and/or F-layer thicknesses. This is demonstrated by the data
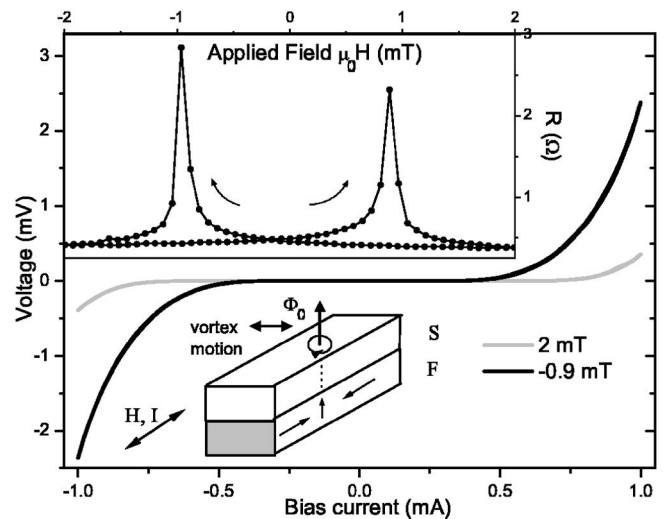

FIG. 4. Current-voltage characteristics at $T=1.8$ K at an applied field $-H_c$ (drawn line) and slightly above $+H_c$ (dotted line) for the GdNi(11)/MoGe(21)/GdNi(11) sample. Inset: $R(H)$ when biasing at 1 mA, above the depinning current. The arrows denote the direction of the field sweep. Also shown is a sketch of the sample configuration, with the directions of applied field, current, and flux inside the F layer (including the domain wall) as indicated.

in Fig. 5 in which MoGe layer is thicker, as well as the inset of Fig. 5 (thicker GdNi). These all show qualitatively similar switching behavior to the original sample. In the case of the thicker MoGe layer some additional features are observed around zero field. These are the two F layers switching independently, (also confirmed by magnetoresistance measurements above T_c—not shown here). This is most likely a combination of a reduction of the direct coupling between the F layers for thicker MoGe, and an increase of the roughness and therefore H_c of the top GdNi layer for a thicker spacer. With thicker GdNi the H_c is reduced, the peaks can shifted to below 0.1 mT leading to a sensitivity in the switching at the
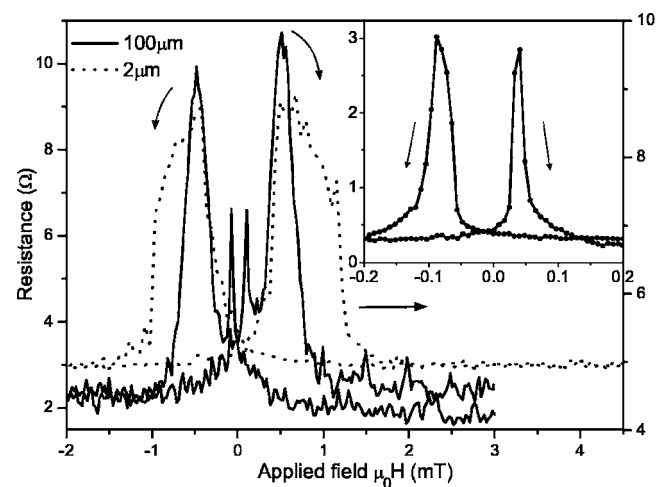

FIG. 5. $R(H)$ curve for GdNi(11)/MoGe(42)/GdNi(11) trilayer at ~5 K for two different wire widths. Inset: GdNi(38)/MoGe(21)/GdNi(38) switching below 0.1 mT at 2.53 K. Arrows denote the direction of the field sweep and the use of the right-hand scale for the 2 μm structure.
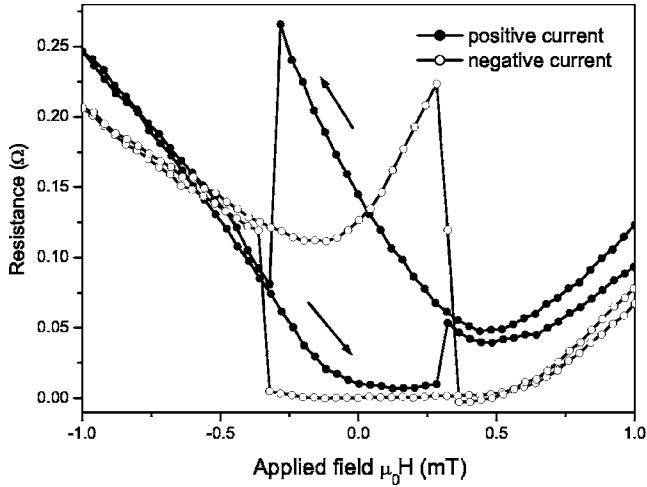
FIG. 6. $R(H)$ for the bilayer MoGe(21)/GdNi(22) at 3.88 K, and current directions as indicated; a positive current is defined as parallel to positive H. The arrows denote the direction of the field sweep.

steepest part of the curve (increasing field sweep) above 60 Ω/mT at an applied field of ~90 μT. In Fig. 5 we also show the effect of patterning wires of different widths. The switching field changes from 100 to 2 μm width due to shape anisotropy, and with it therefore the field at which vortices are present in the MoGe layer. This allows us further control over H_c in complement to varying the thickness of the GdNi layer.

A point of interest is that in bilayer samples the switching behavior is less pronounced and also more complicated, since we now find asymmetry in the peak value of the voltage (resistance), but also asymmetry with respect to the current direction. Field sweeps are shown in Fig. 6 for a bilayer sample MoGe(21)/GdNi(22), at a temperature of 3.88 K, near the bottom of the transition. For positive current (parallel to positive H) a jump rather than a peak is seen at $+H_c$, and a rather broad peak occurs at $-H_c$. We also observe an increasingly resistive background (suppression of the superconductivity) at higher fields. For the other current direction the reverse is the case: a peak in R occurs at $+H_c$ when sweeping from negative H. Unraveling this behavior would need extensive study of the I-V characteristics, which will be for future work. We can, however, identify several differences between trilayers and bilayers. For instance, the bilayer is in fact asymmetric: the order parameter is strongly suppressed at the S/F interface, but not at the free interface, and vortex pinning may actually be sensitive to (inhomogeneities at) the free interface. Also, given the observation of only one resistance peak in the trilayer case it appears that the domain walls couple across the MoGe layer, at least for relatively thin MoGe. We made similar observations of only one resistance peak for trilayers with two different thicknesses of the F layer, such as GdNi(11)/MoGe(21)/GdNi(22). We can speculate that this domain wall coupling both enhances the local flux density in the superconductor and sharpens the switching behavior.

IV. VORTEX FORMATION

We have argued above that the magnetoresistive peaks we observe are due to vortices formed in the S layer above Bloch walls present in the F layer. To make this more compelling, we now estimate whether such vortices can actually be expected to form. For this we use the results from the model discussed recently by Burmistrov and Chtchelkatchev.[12] Basically, they find the amount of flux coming out of a Bloch wall of width δ situated in a ferromagnetic film of thickness d_F characterized by a volume (saturation) magnetization M_s, and from a free energy consideration calculate whether this can lead to the formation of a vortex in a superconducting layer of thickness d_S, characterized by a London penetration depth λ_L, placed on top of the ferromagnet. For the case of a single domain wall they find, for given δ, d_F, d_S, and λ_L, the minimum or critical magnetization M_c needed to overcome the lower critical field H_{c1} of the superconductor. Since in our experiments M_s is a materials constant, it is more convenient to write this condition in terms of a minimum thickness for the F layer, d_F^{min}, which takes the form

$$d_F^{min} = \frac{\lambda H_{c1}}{M_s} \times \begin{cases} 2\lambda/\delta, & (\pi\delta) \ll 4\lambda, \\ 1 - 32G\lambda/(\pi^2\delta), & (\pi\delta) \gg 4\lambda. \end{cases} \quad (1)$$

Here, $\lambda = \lambda_L^2/d_S$ if $d_S < \lambda_L$, otherwise λ equals λ_L; H_{c1} is given by $(\Phi_0/4\pi\mu_0\lambda^2)\ln(\lambda/\xi)$, with ξ the Ginzburg-Landau coherence length and Φ_0 the flux quantum; $G \approx 0.916$ is the Catalan constant, and SI units are used. For MoGe, the relevant values are $\lambda_L \approx 0.7$ μm, which for a 20 nm film yields $\lambda = 24.5$ μm; and $\xi \approx 5$ nm, leading to $H_{c1} \approx 1.8$ A/m, an extremely low value which is due to the combination of a large bulk penetration depth and a small film thickness. For GdNi, the relevant characteristics are M_s and δ. As discussed above, $M_s = 7.8 \times 10^5$ A/m (corresponding to 0.98 T) is relatively large. Values for δ are not exactly known, but the weak magnetocrystalline anisotropy leads to large wall widths, which we take of order 1 μm. The relevant limit is then $\pi\delta \ll 4\lambda$, and Eq. (1) yields $d_F^{min} = 2.9$ nm. For the thicknesses we use, and under the assumption of Bloch walls, the flux from a domain wall is therefore easily large enough to create vortices.

This is the main conclusion from the calculation, but several more remarks are in order. First, it is interesting to note that, in this limit, d_F^{min} does not depend on λ [apart from the logarithmic factor $\ln(\kappa)$], since $H_{c1} \propto 1/\lambda^2$. Then, we have disregarded the effect of the in-plane applied field. In terms of the model, this is allowed since $d_S \ll \lambda$, which means that the field fully penetrates without more than the vacuum contribution to the free energy. Experimentally, it can be noted that misalignment effects are apparently not relevant, since vortices are only created in significant amounts in the domain state of the ferromagnet. Making a rough estimate, an applied field of 2 mT (outside the flux flow peak) under a 1° misalignment yields an induction of 3×10^{-2} A/m, again much smaller than the estimated H_{c1}. Furthermore, we note that, although the flux density from the domain wall is well above the lower critical field $\mu_0 H_{c1}$, it is still much lower than the upper critical field $\mu_0 H_{c2}$. With a typical value of

TABLE I. Comparison of approximate critical thickness of F layer to achieve vortices above a Bloch domain wall for various S and F materials. The column entries show the combination of materials, $\mu_0 M_s$, the estimate for α, the calculated d_F^{min} and the relevant limit for using Eq. (1). Two cases are given for Nb/CuNi, one with the general S-layer thickness of 50 nm, and one with $d_S = 10$ nm, as used in Ref. 11.

System	$\mu_0 M_s$ (T)	δ (μm)	d_F^{min} (nm)	$(\pi\delta)/(4\lambda)$
a-MoGe/a-GdNi	0.98	1	2.9	0.03
Nb/Py	0.7	1	5.7	16
Nb/Co	1.6	0.05	5.9	0.8
Nb/CuNi(50)	0.1	0.25	19.1	0.16
Nb/CuNi(10)	0.1	0.5	20	1.6
YBCO/LCMO	0.75	0.05	51	0.06

$-\mu_0 dH_{c2}/dT \approx 2.5$ T/K, and taking $T - T_c \approx 100$ mK, $\mu_0 H_{c2}(T)$ is found to be ≈ 0.25 T, very much larger than $\mu_0 H_{c1}$. In summary, therefore, the reason that vortices can be observed close to the resistive transition in our MoGe/GdNi system is that the amorphous ferromagnet combines a reasonably large magnetization with a large domain wall width, while the amorphous superconductor combines a large penetration depth with a high upper critical field.

Given these different constraints, it is of interest to consider the possibility of vortex formation in various S/F systems which are currently under investigation as π junctions or spin switches, especially those based on Nb such as Nb/Py, Nb/Co, or Nb/CuNi. The F layers in these combinations are qualitatively different, with Py having large M_s and large δ, Co having large M_s and small δ, and CuNi having small M_s and larger δ. Also considered can be $YBa_2Cu_3O_7$ (YBCO) and $La_{0.7}Ca_{0.3}MnO_3$ (LCMO). For Nb, we use typical values of $d_S = 50$ nm, $\lambda_L = 50$ nm, $\xi = 12$ nm; for YBCO we use $d_S = 50$ nm, $\lambda_L = 180$ nm, $\xi = 2$ nm. The different values for the ferromagnets are given in Table I, together with the computed value for d_F^{min}. This is of course based on the assumption of Bloch and not Néel walls in such thin films, which may not be the case, but the numbers are instructive nonetheless. The table shows that the combination MoGe/GdNi actually yields the lowest value for d_F^{min} due to the combination strong magnet/large domain wall. Still, for the strong magnets the numbers do not vary overmuch; d_F^{min} is typically a few nanometers. For weak CuNi it is significantly larger, which is interesting in view of the observations of Ryazanov et al.[11] They found flux flow behavior in the I-V curves of a Nb wire at in-plane applied fields around the coercive field of a block of 18-nm-thick CuNi on top of a portion of the wire and ascribed the effect to vortices induced in the S layer due to Bloch domain walls in the CuNi. Taking

into account that the Nb layer in their case was only 10 nm thick, the estimated value d_F^{min} is 20 nm, which is roughly the thickness used in the experiment. The Bloch wall scenario for this experiment appears not unreasonable, since the prepared state is in-plane magnetized, while CuNi has a tendency to perpendicular magnetization in this thickness range, as found for CuNi/Cu multilayers.[20] The largest value for d_F^{min} is found for YBCO/LCMO, which is due to the large value of $\ln(\kappa)$ in this system.

V. CONCLUSIONS

We have demonstrated that amorphous F/S/F heterostructures can show large magnetoresistance associated with vortex motion in the S layer, induced by magnetic domains in the F layers. This magnetoresistance can be several tens of ohms change in a field step of a few tens of microteslas due to the combination of weak domain wall and vortex pinning in these amorphous materials. We note that this effect can be a relatively simple test for the presence of Bloch domain walls in a ferromagnetic film. Also, the strong signals may provide a possibility to combine magnetic domain and flux logic[21,22] in a flexible way, since we have demonstrated that both the GdNi thickness and wire widths can be effective tools to tune the fields at which the peaks in flux flow resistivity are observed. That said, we also should mention some problems open for further research. One point we have not touched is the obvious question whether the measured increase in resistance can be tied to flux flow resistivity ρ_{FF} in a quantitative way from the standard formula $\rho_{FF} = \rho_n H/H_{c2}$, with ρ_n the normal state resistance. At the moment we cannot answer that question since, apart from the fact that our measurements have not been performed in the linear regime of the $I(V)$ characteristics where homogeneous flow can be assumed, we know neither the local field, nor the amount of vortices (determined by the domain wall width) between the voltage contacts. Also disregarded in the discussion are possible geometrical effects which would lower the entry field for vortices due to an inhomogeneous current distribution. This touches different questions such as whether this allows smaller values than d_F^{min}, but also whether the nucleation of magnetic domains, through their creation of vortices, actually is facilitated by edges or corners. Fabrication of structures with artificial nucleation points would be an interesting extension of the present work.

[1] A. I. Buzdin, Rev. Mod. Phys. **77**, 935 (2005).

[2] L. R. Tagirov, Phys. Rev. Lett.. **83**, 2058 (1999).

[3] I. Baladié and A. Buzdin, Phys. Rev. B **67**, 014523 (2003).

[4] Y. Fominov, A. A. Golubov, and M. Yu. Kupriyanov, Pis'ma Zh. Eksp. Teor. Fiz. **77**, 609 (2003) [JETP Lett. **77**, 510 (2003)].

[5] J. Y. Gu, C.-Y. You, J. S. Jiang, J. Pearson, Y. B. Bazaliy, and S. D. Bader, Phys. Rev. Lett.. **89**, 267001 (2002).

[6] A. Y. Rusanov, S. Habraken, and J. Aarts, Phys. Rev. B **73**, 060505(R) (2006).

[7] R. J. Kinsey, G. Burnell, and M. G. Blamire, IEEE Trans. Appl. Supercond. **11**, 904 (2001).

[8] Z. Yang, M. Lange, A. Volodin, R. Szymczak, and V. V. Moshchalkov, Nat. Mater. **3**, 793 (2004).

[9] M. Lange, M. J. Van Bael, and V. V. Moshchalkov, Phys. Rev. B **68**, 174522 (2003).

[10] W. Gillijns, A. Yu. Aladyshkin, M. Lange, M. J. Van Bael, and V. V. Moshchalkov, Phys. Rev. Lett. **95**, 227003 (2005).

[11] V. V. Ryazanov, V. A. Oboznov, A. S. Prokof'ev, and S. V. Dubonos, Pis'ma Zh. Eksp. Teor. Fiz. **77**, 43 (2003) [JETP Lett. **77**, 39 (2003)].

[12] I. S. Burmistrov and N. M. Chtchelkatchev, Phys. Rev. B **72**, 144520 (2005).

[13] B. L. T. Plourde, D. J. Van Harlingen, N. Saha, R. Besseling, M. B. S. Hesselberth, and P. H. Kes, Phys. Rev. B **66**, 054529 (2002).

[14] G. J. C. van Baarle, A. M. Troianovski, T. Nishizaki, P. H. Kes and J. Aarts, Appl. Phys. Lett.. **82**, 1081 (2003).

[15] K. Moorjani and J. M. D. Coey, *Magnetic Glasses* (Elsevier, Amsterdam, 1984).

[16] R. Asomoza, A. Fert, I. A. Campbell, A. Liénard and J. P. Rebouillat, J. Phys. F: Met. Phys. **9**, 349 (1979).

[17] We use a density of 6.0×10^{28} at./m^3; see A. Gangulee and R. C. Taylor, J. Appl. Phys. **49**, 1762 (1978).

[18] The magnetization even becomes slightly negative because of the diamagnetic contribution of the Si substrate.

[19] V. Peña, Z. Sefrioui, D. Arias, C. Leon, J. Santamaria, J. L. Martinez, S. G. E. teVelthuis and A. Hoffmann, Phys. Rev. Lett. **94**, 057002 (2005).

[20] A. Ruotolo, C. Bell, C. W. Leung, and M. G. Blamire, J. Appl. Phys. **96**, 512 (2004).

[21] D. A. Allwood, G. Xiong, M. D. Cooke, C. C. Faulkner, D. Atkinson, N. Vernier, and R. P. Cowburn, Science **296**, 2003 (2002).

[22] C. J. Olsen Reichhardt, C. Reichhardt, M. J. Hastings, and B. Jankó, Physica C **404**, 266 (2004).